

Advances in the Application of Photothermal Composite Scaffolds for Osteosarcoma Ablation and Bone Regeneration

Xiaohong Chen,[#] Liqun Yang,[#] Yanfang Wu, Lina Wang, and Huafeng Li*



Cite This: *ACS Omega* 2023, 8, 46362–46375



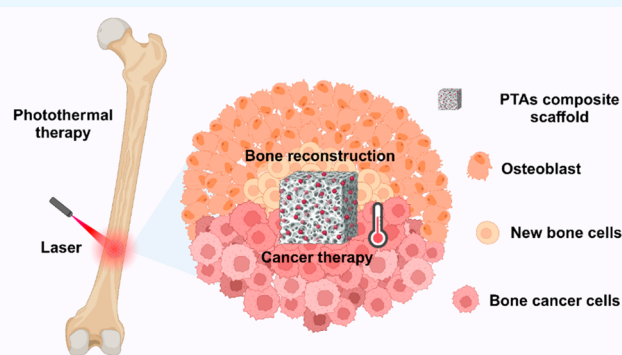
Read Online

ACCESS |

Metrics & More

Article Recommendations

ABSTRACT: Photothermal therapy is a promising approach to cancer treatment. The energy generated by the photothermal effect can effectively inhibit the growth of cancer cells without harming normal tissues, while the right amount of heat can also promote cell proliferation and accelerate tissue regeneration. Various nanomaterials have recently been used as photothermal agents (PTAs). The photothermal composite scaffolds can be obtained by introducing PTAs into bone tissue engineering (BTE) scaffolds, which produces a photothermal effect that can be used to ablate bone cancer with subsequent further use of the scaffold as a support to repair the bone defects created by ablation of osteosarcoma. Osteosarcoma is the most common among primary bone malignancies. However, a review of the efficacy of different types of photothermal composite scaffolds in osteosarcoma is lacking. This article first introduces the common PTAs, BTE materials, and preparation methods and then systematically summarizes the development of photothermal composite scaffolds. It would provide a useful reference for the combination of tumor therapy and tissue engineering in bone tumor-related diseases and complex diseases. It will also be valuable for advancing the clinical applications of photothermal composite scaffolds.



1. INTRODUCTION

Bone cancer, or malignant bone tumor, is a tumor that occurs in the bone or its accessory tissues. It is divided into bone metastasis and primary bone cancer. Bone metastasis refers to secondary malignant bone tumors that metastasize from malignant tumors of other tissues or organs in the body to the bone through blood circulation and the lymphatic system. Osteosarcoma is the most common type of primary bone cancer, occurring mainly in adolescents or adults >60 years. The incidence peak is earlier in girls than in boys because of pubertal growth. The majority of patients present with an excellent overall survival; however, those who develop metastases have survival rates <20%.¹ Traditional treatments, such as surgery, chemotherapy, and radiotherapy, have many side effects and are prone to recurrence and metastasis. The tumor invasion site cannot be repaired by itself,² which brings great pain to patients. In addition, the constant invasion of osteosarcoma into bone can affect bone metabolism and resorb surrounding healthy bone tissue, leading to bone defects.³ This will affect the normal physiological function of patients. Traditional treatment cannot support the bone defect caused by osteosarcoma, nor can it promote the regeneration of the bone defect site, which will affect the normal physiological function of patients. Cancerous bone defects and residual cancer cells are the two key issues related to bone tumor prognosis. Therefore, in the treatment of bone cancer, it is

necessary to construct a multifunctional scaffold that can simultaneously remove cancer cells and repair bone tissue. Based on the above situation, it is urgent to explore new approaches that can treat osteosarcoma and enhance the reconstruction of bone defects resulting from tumor ablation.

Photothermal therapy (PTT) is an effective cancer treatment method that has received wide attention in recent years. Unlike traditional chemotherapy or radiotherapy, it is based on the selective delivery of photothermal agents (PTAs), using their photothermal conversion to produce a thermal effect that kills cancer cells, which has the advantages of localization, high efficiency, and low side effects.⁴ Simply put, it is the use of the photothermal conversion effect of PTAs enriched in tumor sites to generate heat to damage or even ablate surrounding cancer cells under the excitation of near-infrared (NIR) light to eliminate tumor cells and treat cancer.^{5,6} There have been clinical trials reporting good results of PTT in the treatment of prostate tumors and melanoma.⁷ To date, researchers have

Received: September 12, 2023

Revised: October 24, 2023

Accepted: November 14, 2023

Published: November 28, 2023



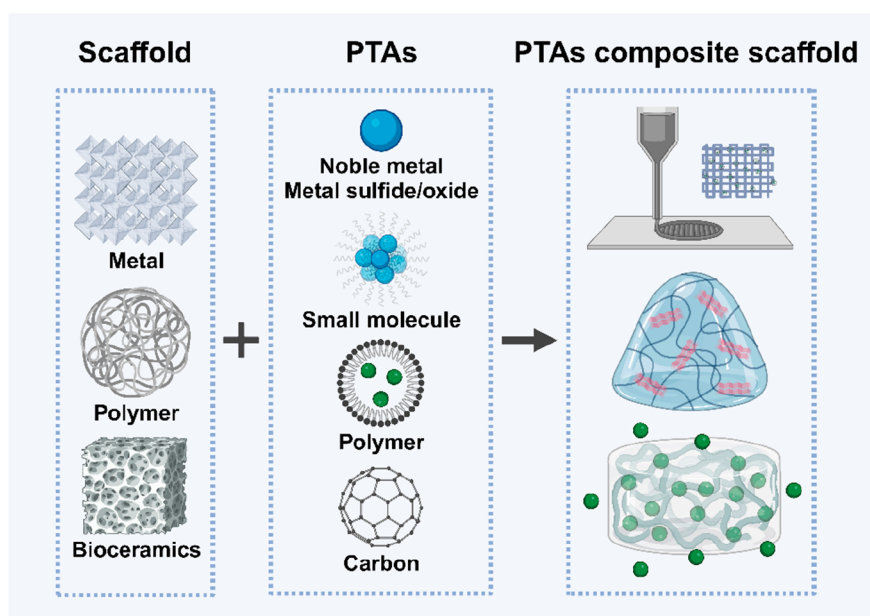


Figure 1. Composition and example diagram of composite photothermal support. Note: this graphic was created with [BioRender.com](https://www.biorender.com).

identified many different types of PTAs, representative of which include polydopamine (PDA),⁸ graphene oxide (GO),⁹ Au nanoparticles (AuNPs),¹⁰ etc., which show excellent performance in photothermal ablation of osteosarcoma. In the clinical practice of osteosarcoma, presumably in the future it will also be a good candidate.

In addition, tissue engineering scaffolds with photothermal effect can promote the regeneration of bone defects after osteosarcoma surgery. First of all, for bone defect regeneration, bone tissue engineering (BTE) has brought new hope.¹¹ Many materials used for bone repair such as metals, ceramics, and polymers can be prepared by tissue engineering techniques like three-dimensional (3D) printing into multiscale bionic structural bioscaffolds that facilitate cellular tissue adhesion.^{12–14} The 3D structure of the stent not only provides an environment for cell adhesion and growth but also functions as a controlled release for drugs and other molecules, which provides conditions for photothermal treatment of osteosarcoma. With the unremitting efforts of researchers, different types of scaffold materials with photothermal effects have emerged, such as photothermal 3D-printed scaffolds and photothermal hydrogels, revealing great potential in osteosarcoma ablation and bone regeneration. In addition, NIR laser-assisted local mild hyperthermia can also significantly accelerate bone tissue regeneration. The photothermal conversion effect can effectively generate thermal stimulation in human tissues noninvasively, thus overcoming the problem of low delivery efficiency of thermal stimulation to specific pathological sites.¹⁵ For bone regeneration, researchers have explored the use of PTAs to induce local thermal stimulation *in vivo* under NIR irradiation at 808 nm. This photothermal stimulation has been shown to increase the expression of heat shock proteins and promote the repair of bone defects, indicating favorable osteogenic activity.^{16,17} Mild PTT can also induce M2 polarization to accelerate the secretion of M2-characteristic cytokines and promote the recruitment of bone mesenchymal stem cells (BMSCs), bone differentiation, and extracellular matrix (ECM) mineralization.¹⁸ There is also a growing number of studies that have shown that BTE scaffolds loaded

with PTAs can achieve a win–win situation for tumor ablation and bone repair.^{19–21} Different types of nano-PTAs are combined with BTE scaffold materials and subsequently implanted into the bone defect site. The tumor ablation effect of the PTAs and the tissue regeneration ability of the scaffold can be fully utilized under laser irradiation of a specific wavelength.

In this paper, we detail the common PTAs, BTE materials, and their preparation methods and characteristics and then summarize the research progress of photothermal composite scaffolds in promoting osteosarcoma ablation and enhancing bone regeneration and discuss their future perspectives in biomedical fields. This review will provide a beneficial reference for the combination of tumor therapy and tissue engineering in osteosarcoma and bone-related tumor diseases and complex diseases. It will also be valuable for advancing the clinical applications of photothermal composite scaffolds.

2. PHOTOTHERMAL COMPOSITE SCAFFOLDS

The photothermal composite scaffold refers to a new composite multifunctional material made of PTAs and BTE scaffolds combined by various technical means, as shown in [Figure 1](#). The 3D structure of the scaffold can mimic the ECM to provide regenerative signals for cells, and the photothermal conversion effect of PTAs can be used to ablate cancer cells.

2.1. Photothermal Agents (PTAs). The key to successful PTT is the selection and use of PTAs, whose conversion efficiency, biocompatibility, and photothermal stability determine the efficacy of tumor ablation.^{22–24} PTAs initiate photothermal effects by absorbing specific light irradiation and converting this energy into heat. NIR light can penetrate deep tissues while causing relatively mild damage. Usually, PTAs in the NIR photobiological window are characterized by low tissue damage, low self-absorption, and high tissue penetration and do not cause significant photodamage due to the concentrated irradiation area of the laser (NIR I: 700–900 nm and NIR II: 1000–1700 nm), and the generated energy is not sufficient to break covalent bonds. Since cancer cells are more heat sensitive than normal cells, PTT can

selectively kill cancer cells without damaging normal tissues and organs,^{25–27} and the heat generated by PTT can further promote normal tissue growth, which is a candidate for clinical treatment of bone cancer.

PTAs are generally nanomaterials, which can be divided into organic, inorganic, and organic–inorganic composite nanomaterials according to their chemical composition.^{28–31} The most commonly used organic PTAs are indocyanine green (ICG) and its analogues, as well as conductive polymers. In 1995, researchers began a series of studies on the tumor ablative ability of ICG, from being discovered for tumor ablation,³² to in situ injection for tumor treatment,^{33,34} and to the development of targeted tumor treatment by preparing ICG-based nanoparticles.³⁵ The typical polymeric PTAs are PDA, polypyrrole (PPy), and semiconducting polymers.^{36–38} They exhibit strong light absorption in the NIR region and have more desirable biophysical properties such as better photostability and biocompatibility in tumor ablation compared to small-molecule dyes. Zeng et al. developed PPy-based nanoparticles (PPy-PEG NPs) with photoacoustic/fluorescence/NIR II multimodal imaging under NIR II by a one-step method. Characterization tests revealed that the nanoparticles exhibited excellent light absorption and photostability, as well as possessing high conversion efficiencies of 33.35% at 808 nm and 41.97% at 1064 nm. Further, *in vivo*, experiments in U87 tumor-bearing mice proved that it could achieve tumor-effective elimination as well as renal metabolism with excellent biosafety.³⁹ It was suggested that PPy-based nanoparticles can exhibit remarkable photothermal effects in tumor environments for PTT application. At the same time, there may be some influence of the size or structure of polymeric materials on their efficacy exertion. Li et al. prepared mesoporous and nonporous PDA nanoparticles (PDA NPs) with similar and uniform particle sizes for comparison and found that the photothermal effect, drug storage capacity, and multiresponsive release characteristics of NIR/pH/H₂O₂ were satisfactory for both carriers. Mesoporous PDA NPs outperformed nonporous PDA NPs in multiple aspects due to the mesoporous structure and higher surface area.⁴⁰ Therefore, the fabrication process of the PTAs is also of great concern for enhancing the photothermal performance. Semiconductor polymer PTA, consisting of a highly extended π -conjugated backbone, is a very attractive optical material in the field of biomedicine.²⁴ The L1057NPs therapeutic system (based on a semiconductor polymer named PTQ) was examined for the potential of NIR II imaging and PTT under 980 nm excitation light. The results exhibited a high mass extinction coefficient of 18 L/(g·cm), and the emission spectrum was almost completely in the NIR II region. There is a peak at 1057 nm with a quantum yield of 1.25% in the NIR II region, which is much higher than most previously reported organic NIR II fluorophores. The investigators also demonstrated that L1057NPs can serve as an excellent photothermal probe to detect tumors in real time.⁴¹

With the development of PTT, researchers have developed a large number of inorganic nano-PTAs for cancer PPT, mainly including carbon-based, transition metal nanomaterials, noble metal nanomaterials, and black phosphorus (BP). Common carbon-based nanomaterials are GO, carbon dots (CDs), and carbon nanotubes,^{42,43} which have high surface area, small size, and excellent electrical and optical properties. Incorporating carbon-based PTAs into 3D porous composite biopolymers or bioceramics (BC) such as chitosan/nanohydroxyapatite can

integrate their PTT effect and tissue regeneration guidance,^{44,45} which has a promising future in bone cancer treatment. Noble metal nanomaterials (AuNPs, AgNPs, PtNPs, PdNPs, etc.) exhibit strong localized surface plasmon resonance,⁴⁶ resulting in high photothermal conversion efficiency. AuNPs have attracted a lot of attention because of their more mature synthesis methods, easy surface modification, and good biocompatibility. Gold nanospheres,⁴⁷ gold nanorods,⁴⁸ gold nanocages,⁴⁹ and gold nanoshells⁵⁰ have demonstrated their unique advantages in photothermal ablation of tumors. Transition metal nanomaterials, including transition metal sulfides (Cu_{2–x}S, MoS₂, etc.)^{51,52} and oxides (Fe₃O₄, MoOx, etc.),⁵³ which are less expensive than noble metals, less cytotoxic, and easier to fabricate, are typically represented by Cu_{2–x}S and Fe₃O₄. The energy band jump of copper ions (Cu²⁺) in Cu_{2–x}S imparts its light absorption properties.^{54,55} In addition, the photothermal conversion efficiency can be effectively improved by adjusting the shape and size of copper-based nanomaterials.^{51,56} Fe₃O₄ has a photothermal effect due to the nonradiative motion of electrons between its different defect sites. As a magnetic nanomaterial, it is capable of enhancing the photothermal effect with the help of a mild alternating magnetic field.⁵⁷ Therefore, transition metal nanomaterials are also widely used in PPT for cancer.

In recent years, researchers have discovered several novel PTAs, such as BP and MXenes, that can be used for PTT of cancer. BP is widely used in PTT because of its wide absorption range in the NIR region, biodegradability, good biocompatibility, and unique layer structure with peelable interlayers.⁵⁸ MXenes are a class of two-dimensional nanomaterials with a high photothermal conversion effect and strong NIR absorption properties.⁵⁹ Since both BPs and MXenes nanosheets have a layered structure and large surface area, they can be loaded with other tumor therapeutic agents or biomolecules for combined therapy.^{60,61} Finally, nanocomposite PTAs such as BPs@Au@Fe₃O₄⁶² can achieve enhanced photothermal conversion efficiency by integrating the advantages of different PTAs and also demonstrate good potential in photothermal treatment of cancer.

Although the above inorganic PTAs usually have the advantages of a large extinction coefficient, easy surface functionalization, high photothermal conversion efficiency, and good photostability, they have limitations such as high cost, poor biodegradability, and long-term toxicity.^{63,64} Organic PTAs are more biodegradable and compatible compared to inorganic PTAs. However, their use in PTT is limited due to their complex synthesis process, poor photothermal stability, and low photothermal conversion efficiency. As the therapeutic effects of single inorganic or organic PTAs are not satisfactory, researchers have shifted their focus toward using a combination of organic and inorganic PTAs to enhance the effectiveness of PTT for cancer treatment.³¹ Studies have reported that organic–inorganic combination PTAs not only integrate the advantages of each but also have synergistic effects. For example, Fe₃O₄@PDA nanocomposite was able to improve T2 imaging contrast in magnetic resonance imaging (MRI) and increase the probability of early osteosarcoma diagnosis. Further experimentation found that Fe₃O₄@PDA particles, when acting as PTAs, result in strong antitumor activity mediation and osteosarcoma lung metastasis prevention under NIR excitation.⁶⁵ The novel MoS₂/PDA-TPP nanocomposite can be dissociated as a pH response to rapidly

release drugs under an acidic tumor microenvironment and improve PTT treatment efficiency. It can also trigger apoptosis by generating reactive oxygen species (ROS) and reducing mitochondrial membrane potential.⁵² Organic–inorganic composite PTAs are capable of multiple responses, which are more valuable for PTT of cancer than single-component PTAs and somewhat also contribute to the early diagnosis of tumors.

2.2. Bone Tissue Engineering (BTE) Scaffolds. The scaffold is one of the elements of tissue engineering and is a 3D biomaterial that provides signals for tissue regeneration. The most important features of scaffolds are interconnected porous structures and high porosity that allow cell adhesion and migration to promote tissue regeneration, proliferation, and differentiation and facilitate cellular nutrient diffusion and waste excretion. The ideal bone tissue scaffold should be biocompatible and biodegradable and have good mechanical properties to act as a structural support for cell growth, allowing the scaffold to stimulate and guide the formation of new tissue for tissue repair after implantation.⁶⁶

Figure 2 shows the common methods for the preparation of BTE scaffolds,⁶⁷ which mainly include electrospinning,⁶⁸ phase

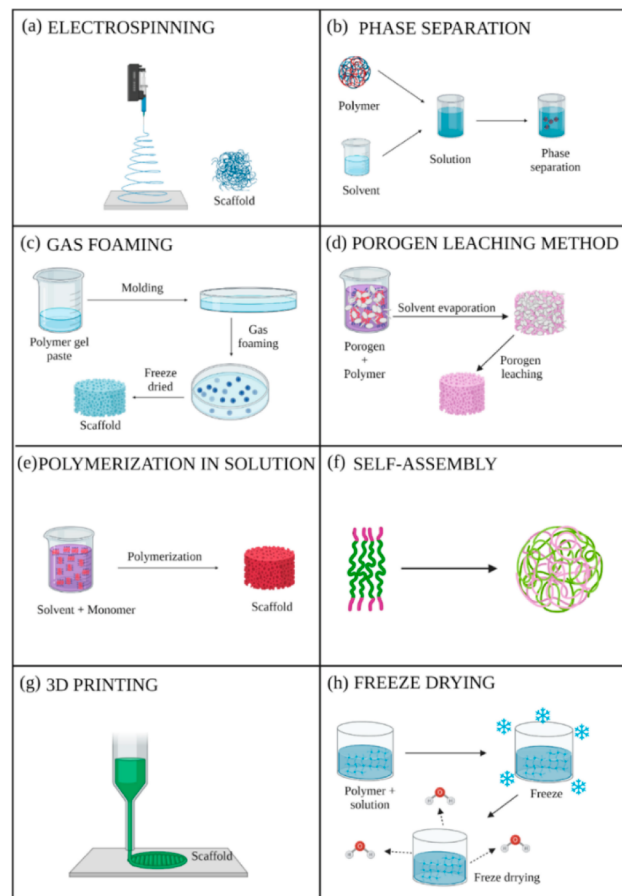


Figure 2. Common methods for the preparation of BTE scaffolds. Reprinted with permission from ref 67. Copyright 2022 Elsevier.

separation,⁶⁹ gas foaming,⁷⁰ porogen leaching method,⁷¹ polymerization in solution,⁷² self-assembly,⁷³ 3D printing,⁷⁴ and freeze-drying.⁷⁵ Each method has its unique technical characteristics. The scaffolds obtained by porogenic leaching and gas foaming techniques are porous in structure, while the pores obtained by gas foaming techniques exhibit a closed state lacking interconnection and no control over the pore

distribution. Recently, it has been reported in the literature that a new solvent-free preparation strategy has been established by combining porogenic agent leaching with supercritical gas foaming technology to overcome the pore size adjustment problem of foaming technology, increased porosity of scaffolds, and enhanced tissue repair capacity.⁷⁶ At the same time, the remaining three bone scaffold fabrication methods show better potential in the field of tissue engineering. The freeze-dried preparations are also porous structures, but their porosity is high, and highly porous scaffolds with certain pore sizes can be prepared by this technique.⁷⁷ Electrostatic spinning is a fiber scaffold prepared by using the action of electrostatic force. The prepared fibers are at the nanometer level⁷⁸ and have high specific surface area and porosity. 3D-printed scaffolds have controllable fiber diameter, pore size, and even pore shape, thereby modifying the mechanical properties and biocompatibility of the scaffold.

As well as the porous and fibrous structures described above, some scaffolds are prepared as hydrogels. Hydrogels are prepared from natural or synthetic polymers as raw materials. The ideal hydrogel has a 3D mesh structure, large porosity, good biodegradability, biocompatibility, certain mechanical properties, and excellent hydrophilicity, which can mimic the ECM structure to promote bone tissue regeneration.^{19,79,80}

Combined with the above manufacturing techniques, a wide range of materials are available for BTE, including inorganic materials, natural polymers, synthetic polymers, and inorganic–organic composites. Among the inorganic materials, the main ones used are metals such as Ti and BC such as Ca–P-based materials (like HA, tricalcium phosphate (TCP), bioactive glasses, and Ca–Si-based materials (such as CaSiO₃ and calomel)). BC is a type of inorganic material that has gained significant attention in research due to its excellent biocompatibility, chemical similarity to natural human bone, ability to promote bone regeneration, and good mechanical strength.^{81–83} Natural polymers, such as collagen, silk fibroin (SF), cold junction gum, chitosan (CS), and alginate, are extensively studied due to their excellent biocompatibility and biodegradability.⁸⁴ Researchers can modulate the structure and mechanical strength of natural polymer scaffolds by cross-linking them in a variety of ways or with chemical modifications. Synthetic polymers are widely used in the manufacture of scaffolds due to their good biocompatibility, biodegradability, strength, stiffness, and ease of processing.⁸⁵ Organic–inorganic composites are a great option for repairing bone defects in patients because they match the components found in natural bone and can anatomically satisfy the repair of the defect site. These composites can also be tailored for specific biological structures and mechanical properties to fully exert their bioactivity, demonstrating great promise in BTE.^{13,86}

2.3. Composite of PTAs and BTE Scaffolds. Researchers have been developing a new type of composite scaffold that combines PTAs and BTE scaffolds. This new scaffold can be implanted at the site of a cancer tumor to enable local treatment with the help of PTT. The scaffold is designed to ablate cancer cells repeatedly in the initial stages of implantation, followed by tissue regeneration to heal the defect caused by the removal of cancer cells. During tissue regeneration, the scaffold provides a bionic growth environment that enhances the healing of tissue defects caused by thermal ablation or resection of the tumor.

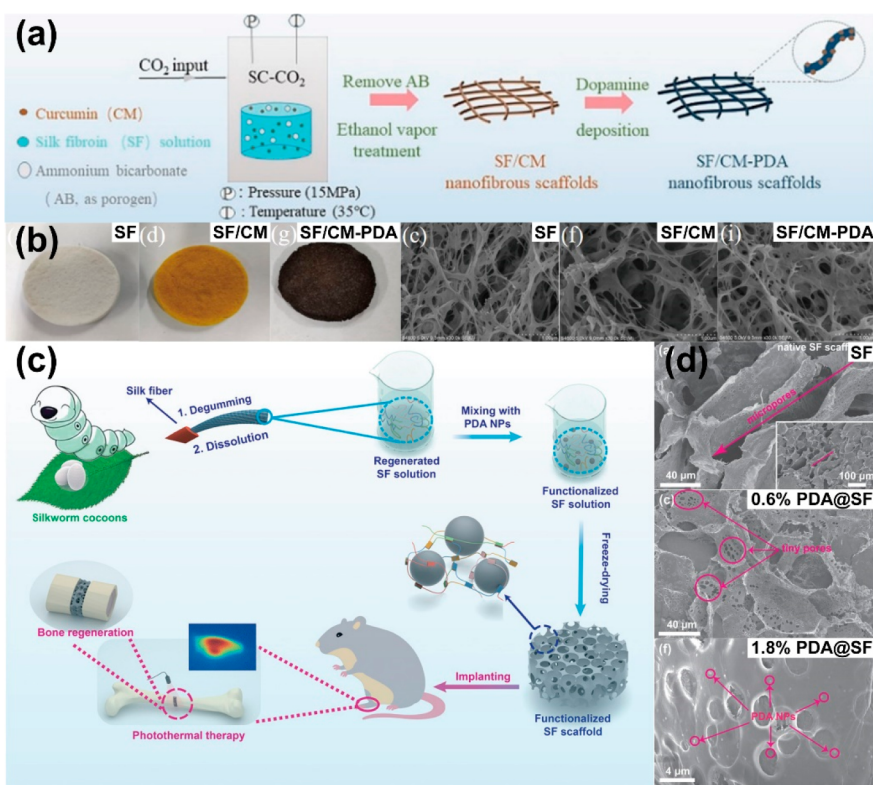


Figure 3. (a) Preparation process of SF/CM-PDA. (b) Photographs of SF, SF/CM, and SF/CM-PDA scaffolds from left to right and corresponding SEM images. Reprinted in parts a and b with permission from ref 89. Copyright 2021 American Chemical Society. (c) Schematic representation of the preparation of PDA@SF scaffolds and their potential applications. (d) Microscopic SEM images of the different components of PDA@SF. Reprinted in parts c and d with permission from ref 90. Copyright 2020 Wiley.

There are two primary methods for combining PTAs with scaffolds: surface modification and internal homogeneous dispersion. Surface modification can involve physically coating the scaffold's surface with PTAs or chemically bonding PTAs to the surface. For instance, PDA–SF-related composite stents can be created using these two composite methods, as illustrated in Figure 3. PDA can be bound to tissue engineering scaffolds in a coating manner due to its unique surface adhesion properties.^{87,88} Figure 3a shows the silk fibroin/curcumin-polydopamine (SF/CM-PDA) composite scaffold obtained by depositing PDA on the surface of a SF/CM nanofiber scaffold,⁸⁹ where the SF/CM scaffold was prepared by supercritical CO₂ technology. The PDA coating was found to improve the hydrophilicity and mechanical strength of the SF/CM scaffold. Figure 3b gives macroscopic overall and microscopic surface SEM images of the composite scaffold. It can be seen that the introduction of CM and PDA leads to a change in the macroscopic color of the scaffold: white–yellow–black, but the microscopic morphology remains largely unchanged, showing interconnected porous and nanofiber structures. Figure 3c shows the process of compounding PDA and SF using internal homogeneous dispersion. The PDA@SF photothermal composite scaffold was obtained by mixing PDA NPs with SF solution and then freeze-drying.⁹⁰ A more uniform distribution of PDA can be observed in SEM. As a result of adding a certain amount of PDA NPs, the microscopic morphology of the composite scaffold was altered. Small pores with a diameter of only a few microns appeared on the micropore walls, which increased the interconnectivity between the micropores and promoted material exchange (Figure 3d). Despite the different ways in which the

photothermal agent was compounded with the BTE scaffold, the composite scaffolds obtained all demonstrated good photothermal conversion capabilities. For the PDA@SF scaffold, as the content of PDA NPs increased, it showed an increasingly strong photothermal effect under laser irradiation. Besides, coculture of the composite scaffold with MC3T3-E1 osteoblasts revealed that PDA NPs could promote cell proliferation to some extent and thus promote bone repair. In the case of the SF/CM-PDA scaffold, in addition to the photothermal ablation of osteosarcoma, CM is also introduced, and the photothermal effect of PDA accelerates the release of CM, thus enhancing its anticancer capacity.

3. APPLICATION OF PHOTOTHERMAL COMPOSITE SCAFFOLDS IN THE TREATMENT OF OSTEOSARCOMA

Treatment of osteosarcoma involves both tumor removal and bone repair. However, traditional single-function biomaterials are no longer sufficient to meet the demand. Therefore, researchers are focusing on developing and applying photothermal composite scaffolds, and the combination of PTT and BTE has gained much attention as a potential treatment for osteosarcoma. Many tissue-engineered scaffold materials have been developed that combine the dual functions of bone tumor ablation and bone tissue regeneration. In this section, we will discuss the latest research progress on different structures and types of photothermal composite scaffolds in PTT for osteosarcoma.

There are various methods to manufacture scaffolds with porous or fibrous structures, leading to more studies on

Table 1. Summary of Typical Porous/Fibrous Photothermal Composite Scaffolds Used in Tumor Therapy and Bone Regeneration

matrix material of the scaffold ^a	type of PTAs ^b	photothermal scaffolds ^c	bone cancer	osteoblast ^d	preparation methods	ref
HA	BP	BPs@HA		BMSCs	3D printing	91
HA/CS	GO	nHA/GO/CS	HOS	MC3T3-E1/hBMSCs	chemical cross-linking	92
	CD	CD/CS/nHA	UMR-106	rBMSCs	freeze-drying	93
HA/CMCS	PDA	PDA/HA/CMCS	UMR-106	mBMSCs	3D printing	8
HA/PEEK	GO	GO/HA/PEEK	MG-63	MC3T3-E1	3D printing	9
TCP	Cu-TCPP	Cu-TCPP/TCP	Saos-2	hBMSCs/HUVECs	3D printing	94
	GO	GO/TCP	MG-63	rBMSCs	3D printing	95
BCP	GO@Fe ₃ O ₄	β -TCP/Fe ₃ O ₄ /GO	MG-63	rBMSCs	3D printing	96
	GNC	GNC/BCP		macrophages/dendritic cells	sintering	97
BG	CuFeSe ₂	CuFeSe ₂ /BG	Saos-2	rBMSCs	3D printing	98
	MoS ₂	MoS ₂ /PLGA/BG	MNNG/HOS	rBMSCs	3D printing	99
	Bi	Bi/BG	Saos-2	rBMSCs	3D printing	100
	CaP	CaBPs@PPF	MCF-7	hBMSCs/QSG-7701	direct encapsulating	101
	HM	DOX-HM-BG	K7M2wt		3D printing	102
	FeSAC	FeSAC-BG	Saos-2	BMSCs	3D printing	103
CaSiO ₃	Fe	Fe-CaSiO ₃	Saos-2	BMSCs	3D printing	104
AKT	Fe ₃ O ₄	Fe ₃ O ₄ -CaO ₂ -AKT	MNNG/HOS	BMSCs	3D printing	105
	Fe ₃ S ₄	Fe ₃ S ₄ -AKT	MG-63	hBMSCs	3D printing	106
	BCN	BCN-AKT	MNNG/HOS	BMSCs	3D printing	107
PCL	SC	SC/PCL	Saos-2	rBMSCs/HUVECs	3D printing	108
PCL-CaCO ₃	CaCuSi ₄ O ₁₀	CaCuSi ₄ O ₁₀ -CaCO ₃ -PCL (CaPCu)	143B/HOS	mBMSCs	3D printing	20
PLGA	Mg	PLGA/Mg	4T1	BMSCs	3D printing	109
	BP	BP/DOX/P24/TCP/PLGA	MG-63	rBMSCs	3D printing	110
TCP/PLGA	PDA/FeMg	PDA/FeMg-NPs/TCP/PLGA	4T1	BMSCs	3D printing	58
PLA	ICG	ICG@DETA/NO-loaded PLA	MG-63	MC3T3-E1	thermally induced phase separation	111
	AuNPs	PCL/PLA/GNFs/AuNPs	MG-63	MC3T3-E1	3D printing	112

^aHA: hydroxyapatite. CS: chitosan. CMCS: carboxymethyl chitosan. PEEK: poly(ether ether ketone). TCP: tricalcium phosphate. BCP: biphasic calcium phosphate. BG: bioactive glasses. AKT: Ca₂MgSi₂O₇. PCL: polycaprolactone. PLGA: polylactic acid–hydroxyacetic acid copolymer. PLA: polylactic acid. ^bBP: black phosphorus. GO: graphene oxide. CD: carbon dot. PDA: polydopamine. Cu-TCPP: copper-coordinated tetra porphyrin (4-carboxyphenyl). GNC: gold nanocages. CaP: calcium phosphate. BCN: boron nitride. SC: SrCuSi₄O₁₀. ICG: indocyanine green. AuNPs: Au nanoparticles. ^cDOX: doxorubicin. ^dBMSCs: bone mesenchymal stem cells. hBMSCs: human bone marrow mesenchymal stem cells. rBMSCs: rat bone marrow mesenchymal stem cells. mBMSCs: mouse bone marrow stromal stem cells. HUVECs: human umbilical vein endothelial cells.

photothermal composite scaffolds for osteosarcoma treatment. Table 1 summarizes representative studies of these scaffolds.

3.1. Photothermal Composite Scaffolds to Inhibit Bone Tumors. Osteosarcoma is the most common type of primary bone tumor in children, adolescents, and young adults, with a poor prognosis, low survival rates, and high rates of metastasis and recurrence. Therefore, it is essential to develop local implants that can selectively kill residual tumor cells.¹¹³

PTT is a noninvasive treatment that has been extensively studied for its potential in treating tumors. One of the main advantages of PTT is that it is cost-effective and can be used for targeted therapy. By using scaffolds that are loaded with PTAs, the therapeutic efficiency can be improved, and the side effects can be reduced through precise spatiotemporal control.¹¹⁴ Xu et al. used a coprecipitation method to introduce GO into tricalcium silicate (tCS) particles, resulting in the formation of tCS/GO composites. The incorporation of GO improved the self-coagulation property of tCS, which enabled it to have excellent performance in NIR light irradiation with remarkable photothermal properties. The temperature of the composite bone cement was regulated by

adjusting the laser power and GO content, and the increase in temperature significantly inhibited the growth of tumor tissue.¹¹⁵ Gel-based scaffolds are a viable option for creating photothermal composite scaffolds that can serve as efficient carriers for PTAs. Yin et al. developed a therapeutic PEEK implant with antimicrobial and tumor thermal ablation properties by cofunctionalizing TOB-containing MXene and GelMA hydrogel. *In vitro* and *in vivo* studies demonstrated that the implant can effectively eliminate osteosarcoma cells using NIR light and also destroy bacteria such as *Escherichia coli* and *Staphylococcus aureus*.¹¹⁶ In addition to scaffolds formed by the substance's function, scaffolds prepared using 3D-printing technology are a common alternative to bone implants. Wang et al. used digital laser processing 3D-printing technology to prepare calcium titanate (CaTiO₃) BC scaffolds. The color of the CaTiO₃ (CaTi) scaffolds intensified with the increase in sintering temperature. The pink CaTi scaffolds had the best compressive strength (13.44 ± 0.99 MPa) and showed good photothermal properties. When exposed to NIR laser irradiation at a rate of 1.32 W/cm², the temperature of the pink CaTi scaffolds exceeds 70 °C. These scaffolds exhibit

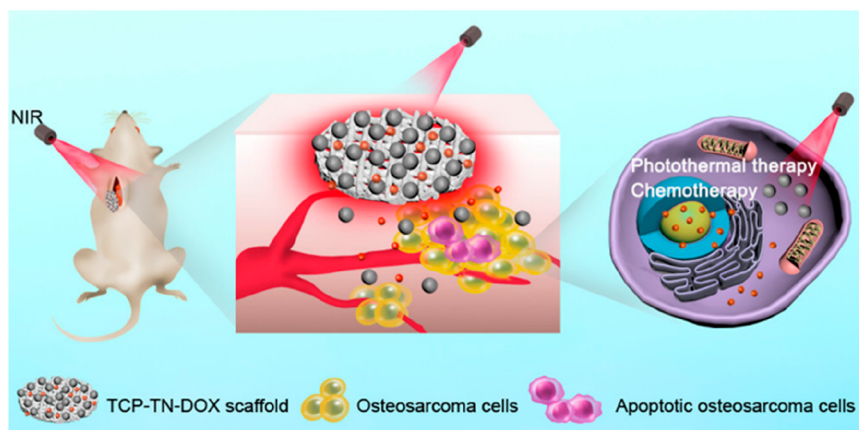


Figure 4. TCP-TN-DOX scaffolds used in photothermal therapy and chemotherapy. Reprinted with permission from ref 118. Copyright 2021 American Chemical Society.

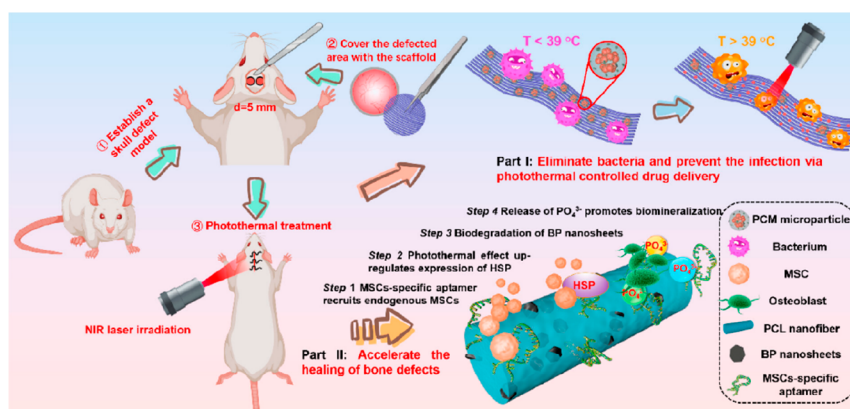


Figure 5. Apt-PCL/BP multifunctional scaffold capable of killing bacteria, recruiting endogenous MSCs, and holding a mild photothermal effect. Reprinted with permission from ref 126. Copyright 2023 American Chemical Society.

excellent photothermal properties, and both *in vivo* and *ex vivo* experiments have shown them to be effective in clearing tumors.¹¹⁷ However, relying solely on photothermal composite scaffolds for localized photothermal treatment of bone tumors is not highly efficient and leads to a high recurrence rate of tumors. The use of scaffolds loaded with different drugs simultaneously is an effective way to enhance the treatment of bone tumors. Dang et al. have developed a multifunctional platform that synergizes the effects of PTT and chemotherapy for treating osteosarcoma (Figure 4). The scaffold's titanium nitride (TiN) and doxorubicin (DOX) content are adjustable by immersing it in solutions with varying concentrations of TiN and DOX. Precise PTT and localized controlled-release chemotherapy have resulted in good therapeutic outcomes both *in vivo* and *ex vivo*.¹¹⁸ He et al. used 3D-printed biodegradable scaffolds incorporated with immunoadjuvant (R837) and modified with niobium carbide (Nb₂C) MXene for treating bone metastases of breast cancer. Since breast cancer often results in systemic metastases, effectively treating breast cancer bone metastasis requires a combined blockade of the PD-L1 checkpoint. This approach can induce dendritic cell recruitment/maturation and cytotoxic T lymphocyte infiltration of the tumor site, which can awaken the immune system and clear the primary as well as metastatic tumors, including distant, lung, and bone metastases. In particular, this combination therapy stimulates the host to build a strong long-term immune memory, which provides long-term

protection against breast cancer.¹¹⁹ Therefore, introducing a multifunctional photothermal composite scaffold presents a wider scope for treating osteosarcoma.

3.2. Photothermal Composite Scaffolds for Bone Repair. BTE has been used to construct bone graft substitutes that can overcome the limitations of limited autologous bone sources, pain in the donor area, immune reactions, and potential infection risks.¹²⁰ The use of efficient, noninvasive, time-controlled PTT is an ideal way to improve the precise treatment of bone defects. With the continuous development of photothermal composite scaffold composition and structural design, better osteogenic properties have been gradually harvested.¹²¹ Liu et al. created a dual-mode delivery system (Figure 5a) for PTHrP-2 (CBP/MBGS/PTHrP-2) using a hydrogel-encapsulated MBG bioscaffold that is responsive to NIR light and temperature. This system is designed to repair and regenerate bone defects. The hydrogel shell made of CDBGn/P(NIPAM-co-NMA), which responds to light and heat, can precisely control the release of PTHrP-2 from the mesopores of MBGS at slow or pulsed rates. This continuous release promotes the proliferation and osteogenic differentiation of bone mesenchymal stem cells (BMSCs). The controlled concentration of PTHrP-2 is sufficient for the formation of endothelial tubes by HUVECs at the bone defect site. Additionally, the interconnected porous structure of MBGS provides enough space and conditions for the recruitment, proliferation, and differentiation of osteogenesis-

associated cells.¹²² PCL is a commonly used BTE material in 3D-printed scaffolds. Such scaffolds can be used for multifunctional bone repair and can be enhanced bioactively and made to deliver drugs intelligently.¹²³ Xue et al. utilized 3D-printed PCL scaffolds that were encapsulated with nano-CuS-PEG soft hydrogel, referred to as CuS-PEG-PCL scaffolds, loaded with dexamethasone sodium phosphate (Dexp). The PCL scaffolds provided excellent mechanical properties, while CuS nanoparticles cross-linked PEG hydrogel (CuS-PEG-hydrogel) provided stable soft elasticity and excellent photothermal properties to the PCL-based scaffolds. On-demand drug release and local warming were achieved by 1064 nm NIR light to promote osteogenic differentiation. Experiments demonstrated that BMSCs implanted in D-CuS-PEG-PCL scaffolds achieved good bone regeneration effects both *in vitro* and *in vivo* after being irradiated with NIR light.¹²⁴ In addition, photothermal composite PCL-based tissue engineering scaffolds can have unexpected effects on periosteum repair. Based on the structural and functional properties of natural periosteum, Li et al. developed a bilayered PCL nanofibrous membrane (PCL/Nd@WH) with a surface-orientated structure by combining electrostatic spinning and laser etching technologies and loaded Nd@WH nanoparticles in it. The structured nanofiber membrane containing Nd@WH nanoparticles induced the formation of endogenous periosteum by releasing magnesium ions (Mg^{2+}). The composite periosteum had regenerative properties, as confirmed by experimental detection of increased levels of factors such as VEGF and NGF.¹²⁵ To ensure the safe and effective use of photothermal treatment, it is essential to consider the temperature control of its application. Excessively high temperatures can lead to damage to normal tissues surrounding the lesion. To address this issue, Zhang developed a multifunctional nanofiber scaffold (Figure 5b) using a stepwise treatment approach, which effectively treats the lesion while minimizing the harmful effects of high temperatures. The antibiotic vancomycin was loaded into the PCM particles by coaxial electrospinning, which could be triggered to be released by NIR light (808 nm) to prevent early bacterial proliferation. The surface of electrospun PCL/BP nanofiber scaffolds was modified with nucleic acid aptamers to recruit endogenous MSCs. BP NSs were loaded into the nanofibers, which provided mild thermal therapy under NIR light irradiation and facilitated osteogenesis. In addition, this method increased the expression of Heat Shock Proteins (HSPs), which helped to improve bone regeneration. The effectiveness of this technique was demonstrated in a rat cranial defect model.¹²⁶ Whether it is the mechanical effect of scaffolds on bone tissue, the repair performance of thermotherapy on bone defects, or the delivery and control of photothermal composite scaffolds for the delivery of functionally relevant drugs or factors for bone repair, based on the efficacy of photothermal composite scaffolds for bone repair and the inhibitory property of photothermal itself for osteosarcoma, it provides a new option for tissue regeneration after osteosarcoma treatment.

3.3. Bone Repair Function of Photothermal Composite Scaffolds in Osteosarcoma Treatment. Bone tumors have a very high morbidity and mortality rate, which seriously affects the quality of life of patients. Despite the high selectivity, low toxicity, and high tumor treatment efficiency of PTT, nanomaterials usually cannot repair bone defects caused by bone tumor surgery.¹²⁷ To address this need for postoperative bone repair, researchers are focusing on

developing photothermal composite scaffolds that can promote regeneration and have therapeutic effects in osteosarcoma treatment.^{128,129} Zhang et al. constructed a novel bone scaffold with nanohydroxyapatite (n-HA), MXene nanosheets, and $g-C_3N_4$. The scaffold has excellent photothermal properties and can be rapidly heated up to 45 °C in about 3 min under 808 nm laser irradiation. The combination of $Ti_3C_2T_x$ and $g-C_3N_4$ promotes electron generation, reduces the band gap width, and improves ROS generation. In addition, the doping of n-HA had an inhibitory effect on osteosarcoma cells as well as the function of promoting the proliferation, osteogenic differentiation, and related osteogenic gene expression of BMSCs, thus promoting new bone formation after osteosarcoma treatment.¹³⁰ Considering the impact on normal tissues, lowering the action temperature of PTT and improving the functionality of bone tissue-engineered scaffolds can achieve healthy performance of PTT in osteosarcoma treatment. Pektas et al. developed a bifunctional thermally regenerative 3D aerogel composite scaffold by combining photo-cross-linked SF biopolymer and MXene (Ti_3C_2) two-dimensional nanosheets. The 3D-printed self-assembly-driven and photo-cross-linked SF-based aerogel coating loaded with Sorafenib features drug NIR-responsive release, promotion of osteoblastic cell growth and proliferation, and enhancement of bone mineral deposition in both acidic and neutral media. These findings suggest that thermal regeneration aerogel could play a vital role in bone regeneration after thermal ablation of osteosarcoma.¹³¹

Bone tissue contains various metal elements, which play a crucial role in the bone regeneration process. The commonly used metal ions for bone regeneration are Mg^{2+} , calcium ions (Ca^{2+}), strontium ions (Sr^{2+}), zinc ions (Zn^{2+}), lithium ions (Li^+), manganese ions (Mn^{2+}), Cu^{2+} , cobalt ions (Co^{2+}), cerium ions (Ce^{3+}), iron ions (Fe^{3+}), and silver ions (Ag^+). They play a vital role in different aspects of bone metabolism, such as osteoblast and osteoclast differentiation and activity, bone mineralization, and angiogenesis.¹³² Liu et al. manufactured bioactive glass-ceramic (BGC) scaffolds using 3D printing and with Cu, Fe, Mn, and Co elements, which had a photothermal effect and osteogenic differentiation ability. They conducted a study to investigate the photothermal antitumor effect and osteogenic activity of these scaffolds. The study confirmed that the final temperature of the dopant-element scaffolds could be controlled by varying the type and content of the dopant elements and the laser power density. Among them, 5Cu-BGC, 5Fe-BGC, and 5Mn-BGC-induced thermotherapy were effective in killing tumor cells *in vitro* and inhibiting tumor growth *in vivo*. Moreover, the 5Fe-BGC and 5Mn-BGC scaffolds promoted the adhesion of rabbit bone marrow mesenchymal stem cells (rBMSCs), and the ionic products released from the doping element scaffolds significantly stimulated osteoblasts' osteogenic differentiation. These results indicate that combining metal ions with tissue-engineered scaffolds is an effective solution for constructing bioactive ion-functionalized scaffolds for treating bone tumors.¹³³ Zhang et al. printed β -tricalcium phosphate/ $SrCuSi_4O_{10}$ (β -TCP/SC) nanosheet composites as the shells of hollow microfilaments (denoted as hTCP/SC), and core-shell scaffolds were constructed with adriamycin-loaded gelatin as the core of the microfilaments. The NIR-responsiveness of SC nanosheets endowed the scaffolds with photothermal functionality. Meanwhile, the generated high temperature prompted the DOX-loaded gelatin to transform from gel to

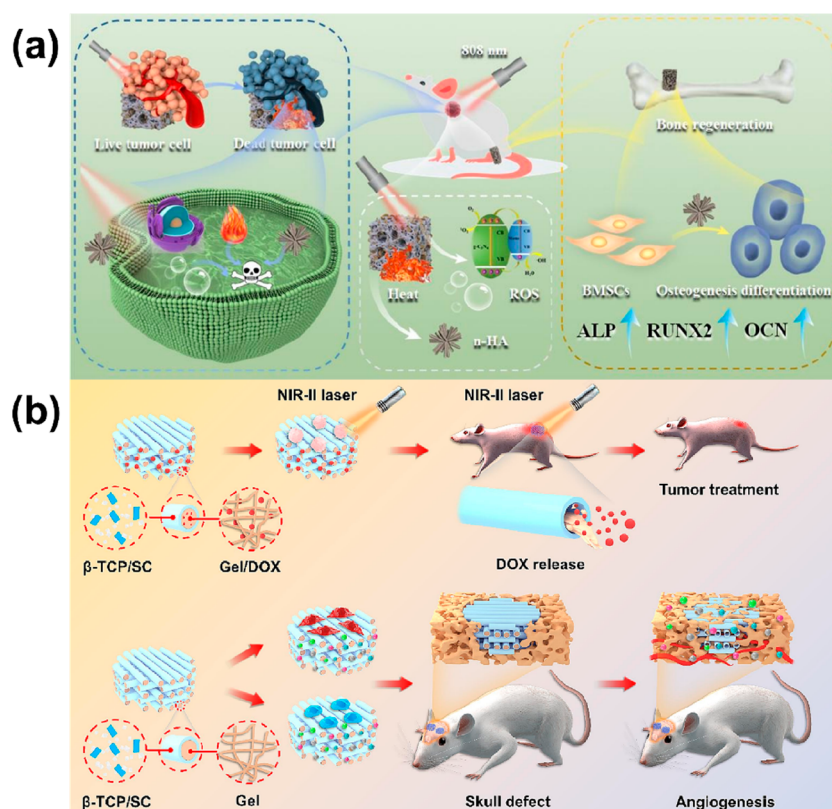


Figure 6. (a) HA/C@M-8/0.6 scaffold for tumor ablation and new bone formation. Reprinted with permission from ref 130. Copyright 2023 Elsevier. (b) 3D-printed gelatin/bioceramics core/shell composite scaffolds for bone tumor chemo-photothermal therapy with triggered drug release for tumor treatment and enhanced bone regeneration. Reprinted with permission from ref 134. Copyright 2023 Elsevier.

sol, releasing DOX and forming a chemo-photothermal synergistic treatment for osteosarcoma cells (Figure 6). With the degradation of gelatin, hollow TCP/SC scaffolds that provide spatial and architectural guidance for nutrient transport and cell migration are formed. Meanwhile, the degradation of SC nanosheets generates bioactive ions (such as Sr, Cu, and Si) that can promote the process of angiogenesis and bone regeneration.¹³⁴ The combination of biodegradable scaffolds with metallic elements in BTE has led to the development of photothermal composite scaffolds that are suitable for *in vivo* implants. Based on this, Gu et al. used a melt-quenching method to prepare iron-doped and copper-doped phosphate glasses. They can thermally ablate tumor cells to produce effective degradation *in vivo*, while the released ions can promote osteoblast proliferation for bone repair. The photothermal properties of the composite scaffolds were able to be controlled by laser power density, elemental doping content, and glass melting temperature. In cellular experiments, it was found that the high temperature induced by the photothermal effect of PGFe5-1100 and PGCu5-1100 could effectively kill MG63 cells, whereas PGFe5-1100 supported the proliferation and osteogenic differentiation of MC3T3-E1 cells. After being immersed in Tris-HCl solution for 28 days, the degradation rates of PGFe5-1100 and PGCu5-1100 were 1.13% and 3.26%, respectively. During the degradation process, P, Ca, Na, and Fe/Cu ions were released. Compared to conventional PTAs, phosphate glass containing transition metal elements accomplished tumor eradication, bone regeneration, and degradation with better biosafety and bioactivity.¹³⁵ Moreover, the ease of modification of biomaterials endows bone tissue scaffolds with richer

functionalities. Kong et al. used gadolinium-doped polydopamine nanoparticles (PDA@Gd), which exhibited excellent biocompatibility and photothermal properties, as scaffold material. They achieved targeted delivery of nanoparticles to bone tumors through bone-targeting peptide modification using eight aspartic acids (D8) and RGD-derived peptide RGDfRGDfC (RGD2). In addition to targeting the tumor, the RGD2 peptide on the surface of PDA@Gd nanoparticles prevented osteolysis by inhibiting osteoclast activation. The PDA@Gd nanoparticles delivered have a dual-modality imaging feature, which includes photoacoustic imaging (PAI) and magnetic resonance imaging (MRI), making it an efficient diagnostic tool for osteosarcoma treatment and further bone restoration.¹³⁶ Therefore, combining clinical needs, disease characteristics, and problems, choosing the right photothermal composite scaffolds or appropriately designed functional scaffolds brings new hope for the complex treatment of osteosarcoma and becomes a more convenient and promising opportunity.

4. CONCLUSION AND PROSPECTS

This paper systematically summarizes the application of photothermal composite scaffolds in osteosarcoma ablation and bone regeneration in recent years from the perspective of common PTAs, BTE materials, and manufacturing methods. Unlike conventional bone cancer treatment methods, these composite scaffolds can be implanted or even injected into bone tumor sites to eliminate tumor cells by the photothermal conversion effect induced by PTAs loaded on the scaffolds. In addition, the bone tissue-engineered scaffold's structure supports bone cell growth and tissue repair of the defect site

after ablation. Meanwhile, synergistic treatment strategies, such as ROS therapy and pharmacological treatment, have been developed to improve the treatment effects or reduce the adverse reactions of osteosarcoma.

At present, many photothermal composite scaffolds have been successfully developed for osteosarcoma treatment and bone regeneration, but there are fewer studies on their application at the clinical stage, and there are many problems that need to be addressed. First, the penetration depth of PTAs limits their clinical applications. Most PTAs for PPT are in the NIR I region, and only a few investigators have developed photothermal scaffolds with stronger penetration depth (e.g., CaCuSi₄O₁₀–CaCO₃–PCL scaffold and SC/PCL) and which have shown excellent performance under NIR II laser irradiation. Therefore, it is necessary to develop novel PTAs for NIR II biological windows. As well, the development of new organic–inorganic composite PTAs is valuable for the treatment of osteosarcoma. Composite PTAs not only integrate their respective advantages but also have synergistic effects. Second, the effects of the most photothermal composite scaffolds for bone tumors and bone tissue reconstruction are usually studied separately and cannot mimic the actual situation in disease treatment, so the selection of suitable animal models is important to advance the clinical application of these composite scaffolds. Third, composite scaffolds' synergistic treatment strategies should be further developed. Currently, PTT/chemotherapy, PTT/photodynamic therapy (PDT), and PTT/ROS therapy have successfully improved the therapeutic effect of tumors, but other therapeutic modalities can be developed and utilized synergistically, such as immunotherapy, acoustic power therapy, and starvation therapy. Finally, considering infections, bleeding, etc., the future development of scaffolds may need to be given more functions, such as the introduction of antibacterials, coagulation, and other bioactive substances in photothermal stents to enhance the therapeutic efficacy.

Despite the many challenges in the clinical application of photothermal composite scaffolds, their great promise in cancer treatment has encouraged researchers to investigate further and translate them into clinical applications.

AUTHOR INFORMATION

Corresponding Author

Huafeng Li – Department of General Surgery, Haining Central Hospital, Jiaxing 314400, China; orcid.org/0009-0001-9134-6183; Email: lhf_052@163.com

Authors

Xiaohong Chen – Department of Pediatric Internal Medicine, Haining Central Hospital, Jiaxing 314400, China
Liqun Yang – Department of Nursing, Tongxiang Traditional Chinese Medicine Hospital, Jiaxing 314500, China
Yanfang Wu – Department of Hematology, The First People's Hospital of Fuyang Hangzhou, Hangzhou 311400, China
Lina Wang – Department of Internal Medicine, The Second People's Hospital of Luqiao Taizhou, Taizhou 318058, China

Complete contact information is available at:
<https://pubs.acs.org/10.1021/acsomega.3c06944>

Author Contributions

[#]The manuscript was written through the contributions of all authors. All authors have approved the final version of the manuscript. X.C. and L.Y. contributed equally to this paper.

Notes

The authors declare no competing financial interest.

ACKNOWLEDGMENTS

This work was supported by Zhejiang Province Science and Technology Development Funds of Traditional Chinese Medicine (2021ZB245) and the Project of Zhejiang Province Education Committee (Y202249376).

REFERENCES

- (1) Beird, H. C.; Bielack, S. S.; Flanagan, A. M.; Gill, J.; Heymann, D.; Janeway, K. A.; Livingston, J. A.; Roberts, R. D.; Strauss, S. J.; Gorlick, R. Osteosarcoma. *Nat. Rev. Dis. Primers* **2022**, *8* (1), 77.
- (2) Gill, J.; Gorlick, R. Advancing therapy for osteosarcoma. *Nat. Rev. Clin. Oncol.* **2021**, *18* (10), 609–624.
- (3) Machoň, V.; Vlachopoulos, V.; Beňo, M. Reconstruction of Temporomandibular Joint and Skull Base Defect Following Osteosarcoma Resection. *Journal of Craniofacial Surgery* **2022**, *33* (7), e667–e669.
- (4) Liu, Y.; Bhattarai, P.; Dai, Z.; Chen, X. Photothermal therapy and photoacoustic imaging via nanotheranostics in fighting cancer. *Chem. Soc. Rev.* **2019**, *48* (7), 2053–2108.
- (5) Pan, H.; Zhang, C.; Wang, T.; Chen, J.; Sun, S.-K. In Situ Fabrication of Intelligent Photothermal Indocyanine Green-Alginate Hydrogel for Localized Tumor Ablation. *ACS Appl. Mater. Interfaces* **2019**, *11* (3), 2782–2789.
- (6) Ding, F.; Gao, X.; Huang, X.; Ge, H.; Xie, M.; Qian, J.; Song, J.; Li, Y.; Zhu, X.; Zhang, C. Polydopamine-coated nucleic acid nanogel for siRNA-mediated low-temperature photothermal therapy. *Biomaterials* **2020**, *245*, 119976.
- (7) Rastinehad, A. R.; Anastos, H.; Wajswol, E.; Winoker, J. S.; Sfakianos, J. P.; Doppalapudi, S. K.; Carrick, M. R.; Knauer, C. J.; Taouli, B.; Lewis, S. C.; et al. Gold nanoshell-localized photothermal ablation of prostate tumors in a clinical pilot device study. *Proc. Natl. Acad. Sci. U. S. A.* **2019**, *116* (37), 18590–18596.
- (8) Yao, M.; Zou, Q.; Zou, W.; Xie, Z.; Li, Z.; Zhao, X.; Du, C. Bifunctional scaffolds of hydroxyapatite/poly(dopamine)/carboxymethyl chitosan with osteogenesis and anti-osteosarcoma effect. *Biomater. Sci.* **2021**, *9* (9), 3319–3333.
- (9) Zhu, C.; He, M.; Sun, D.; Huang, Y.; Huang, L.; Du, M.; Wang, J.; Wang, J.; Li, Z.; Hu, B.; et al. 3D-Printed Multifunctional Polyetheretherketone Bone Scaffold for Multimodal Treatment of Osteosarcoma and Osteomyelitis. *ACS Appl. Mater. Interfaces* **2021**, *13* (40), 47327–47340.
- (10) Xiong, S. R.; Xiong, G. S.; Li, Z. H.; Jiang, Q.; Yin, J.; Yin, T.; Zheng, H. Gold nanoparticle-based nanoprobes with enhanced tumor targeting and photothermal/photodynamic response for therapy of osteosarcoma. *Nanotechnology* **2021**, *32* (15), 155102.
- (11) Peng, Y.; Zhuang, Y.; Liu, Y.; Le, H.; Li, D.; Zhang, M.; Liu, K.; Zhang, Y.; Zuo, J.; Ding, J. Bioinspired gradient scaffolds for osteochondral tissue engineering. *Exploration* **2023**, *3* (4), 20210043.
- (12) Pan, T.; Song, W. J.; Xin, H. B.; Yu, H. Y.; Wang, H.; Ma, D. D.; Cao, X. D.; Wang, Y. J. MicroRNA-activated hydrogel scaffold generated by 3D printing accelerates bone regeneration. *Bioact. Mater.* **2022**, *10*, 1–14.
- (13) van der Heide, D.; Cidonio, G.; Stoddart, M. J.; D'Este, M. 3D printing of inorganic-biopolymer composites for bone regeneration. *Biofabrication* **2022**, *14* (4), 042003.
- (14) Sun, X.; Yang, J.; Ma, J.; Wang, T. C.; Zhao, X.; Zhu, D.; Jin, W. J.; Zhang, K.; Sun, X. Z.; Shen, Y. L.; et al. Three-dimensional bioprinted BMSCs-laden highly adhesive artificial periosteum containing gelatin-dopamine and graphene oxide nanosheets promoting bone defect repair. *Biofabrication* **2023**, *15* (2), 025010.

- (15) Zheng, M.; Guo, R.; Liu, Z.; Wang, B.; Meng, L.; Li, F.; Li, T.; Luo, Y. MoS₂ intercalated p-Ti3C₂ anode materials with sandwich-like three dimensional conductive networks for lithium-ion batteries. *J. Alloys Compd.* **2018**, *735*, 1262–1270.
- (16) Yang, K.; Zhao, S.; Li, B.; Wang, B.; Lan, M.; Song, X. Low temperature photothermal therapy: Advances and perspectives. *Coord. Chem. Rev.* **2022**, *454*, 214330.
- (17) Chen, J.; Ning, C.; Zhou, Z.; Yu, P.; Zhu, Y.; Tan, G.; Mao, C. Nanomaterials as photothermal therapeutic agents. *Prog. Mater. Sci.* **2019**, *99*, 1–26.
- (18) Li, B.; Liu, F.; Ye, J.; Cai, X.; Qian, R.; Zhang, K.; Zheng, Y.; Wu, S.; Han, Y. Regulation of Macrophage Polarization Through Periodic Photo-Thermal Treatment to Facilitate Osteogenesis. *Small* **2022**, *18* (38), 2202691.
- (19) Liu, X.; Zhang, Y.; Wu, H.; Tang, J.; Zhou, J.; Zhao, J.; Wang, S. A conductive gelatin methacrylamide hydrogel for synergistic therapy of osteosarcoma and potential bone regeneration. *Int. J. Biol. Macromol.* **2023**, *228*, 111–122.
- (20) He, C.; Dong, C.; Yu, L.; Chen, Y.; Hao, Y. Ultrathin 2D Inorganic Ancient Pigment Decorated 3D-Printing Scaffold Enables Photonic Hyperthermia of Osteosarcoma in NIR-II Biowindow and Concurrently Augments Bone Regeneration. *Adv. Sci. (Weinheim, Ger.)* **2021**, *8* (19), e2101739.
- (21) Yang, Z.; Li, Z.; Zhao, Y.; Zhao, Y.; Li, X.; He, L.; Zvyagin, A. V.; Yang, B.; Lin, Q.; Ma, X. Lotus Seedpod-Inspired Crosslinking-Assembled Hydrogels Based on Gold Nanoclusters for Synergistic Osteosarcoma Multimode Imaging and Therapy. *ACS Appl. Mater. Interfaces* **2022**, *14* (30), 34377–34387.
- (22) Lv, F.; Fan, X.; Liu, D.; Song, F. Photothermal agents based on small organic fluorophores with intramolecular motion. *Acta Biomater.* **2022**, *149*, 16–29.
- (23) Yang, X.-Z.; Wen, L.-F.; Xu, G.; Lin, H.-H.; Wang, S.; Liu, J.-Y. Multifunctional organic nanomaterials with ultra-high photothermal conversion efficiency for photothermal therapy and inhibition of cancer metastasis. *Bioorg. Chem.* **2023**, *130*, 106220.
- (24) Zhang, Z.; Li, W.; Liu, Y.; Fang, X.; Wu, C. Semiconducting Polymer Nanoparticles in the Second Near-Infrared Region for Biomedical Imaging and Therapy. *Adv. Opt. Mater.* **2023**, *11* (11), 2202052.
- (25) Lyu, Y.; Li, J.; Pu, K. Second Near-Infrared Absorbing Agents for Photoacoustic Imaging and Photothermal Therapy. *Small Methods* **2019**, *3* (11), 1900553.
- (26) Wang, Z.; Wang, M.; Wang, X.; Hao, Z.; Han, S.; Wang, T.; Zhang, H. Photothermal-based nanomaterials and photothermal-sensing: An overview. *Biosens. Bioelectron.* **2023**, *220*, 114883.
- (27) Fu, L.; Jin, W.; Zhang, J.; Zhu, L.; Lu, J.; Zhen, Y.; Zhang, L.; Ouyang, L.; Liu, B.; Yu, H. Repurposing non-oncology small-molecule drugs to improve cancer therapy: Current situation and future directions. *Acta Pharm. Sin. B* **2022**, *12* (2), 532–557.
- (28) Yu, Z.; Chan, W. K.; Zhang, Y.; Tan, T. T. Y. Near-infrared-II activated inorganic photothermal nanomedicines. *Biomaterials* **2021**, *269*, 120459.
- (29) Zhou, W.; Du, M.; Wang, J.; Zhang, X.; Liang, T.; Xie, C.; Fan, Q. Organic nanomaterials for near-infrared light-triggered photothermal/thermodynamic combination therapy. *Dyes Pigm.* **2022**, *205*, 110499.
- (30) Shang, H.; Wu, J.; Liu, X.; Tong, Y.; He, Y.; Huang, Q.; Xia, D.; Peng, E.; Chen, Z.; Tang, K. Second near-infrared nanomaterials for cancer photothermal immunotherapy. *Mater. Today Adv.* **2023**, *17*, 100339.
- (31) Yang, S.; Yang, P.; Xie, Y.; Zhang, B.; Lin, J.; Fan, J.; Zhao, Z. Organic-inorganic hybrid photothermal nanomaterials for combined photothermal and chemotherapy therapy of tumors under the dual biological window. *J. Mater. Sci.* **2021**, *56* (32), 18219–18232.
- (32) Chen, W. R.; Adams, R. L.; Bartels, K. E.; Nordquist, R. E. Chromophore-Enhanced In-Vivo Tumor-Cell Destruction Using an 808-Nm Diode-Laser. *Cancer Lett. (N. Y., NY, U. S.)* **1995**, *94* (2), 125–131.
- (33) Chen, W. R.; Adams, R. L.; Higgins, A. K.; Bartels, K. E.; Nordquist, R. E. Photothermal effects on murine mammary tumors using indocyanine green and an 808-nm diode laser: An in vivo efficacy study. *Cancer Lett. (N. Y., NY, U. S.)* **1996**, *98* (2), 169–173.
- (34) Chen, W. R.; Adams, R. L.; Carubelli, R.; Nordquist, R. E. Laser-photosensitizer assisted immunotherapy: A novel modality for cancer treatment. *Cancer Lett. (N. Y., NY, U. S.)* **1997**, *115* (1), 25–30.
- (35) Chen, Z.; Zhao, P.; Luo, Z.; Zheng, M.; Tian, H.; Gong, P.; Gao, G.; Pan, H.; Liu, L.; Ma, A.; et al. Cancer Cell Membrane-Biomimetic Nanoparticles for Homologous-Targeting Dual-Modal Imaging and Photothermal Therapy. *ACS Nano* **2016**, *10* (11), 10049–10057.
- (36) Liu, S.; Pan, J.; Liu, J.; Ma, Y.; Qiu, F.; Mei, L.; Zeng, X.; Pan, G. Dynamically PEGylated and Borate-Coordination-Polymer-Coated Polydopamine Nanoparticles for Synergistic Tumor-Targeted, Chemo-Photothermal Combination Therapy. *Small* **2018**, *14* (13), 1703968.
- (37) Zha, Z.; Yue, X.; Ren, Q.; Dai, Z. Uniform Polypyrrole Nanoparticles with High Photothermal Conversion Efficiency for Photothermal Ablation of Cancer Cells. *Adv. Mater.* **2013**, *25* (5), 777–782.
- (38) Jiang, Y.; Li, J.; Zhen, X.; Xie, C.; Pu, K. Dual-Peak Absorbing Semiconducting Copolymer Nanoparticles for First and Second Near-Infrared Window Photothermal Therapy: A Comparative Study. *Adv. Mater.* **2018**, *30* (14), 1705980.
- (39) Zeng, W.; Wu, X.; Chen, T.; Sun, S.; Shi, Z.; Liu, J.; Ji, X.; Zeng, X.; Guan, J.; Mei, L.; et al. Renal-Clearable Ultrasmall Polypyrrole Nanoparticles with Size-Regulated Property for Second Near-Infrared Light-Mediated Photothermal Therapy. *Adv. Funct. Mater.* **2021**, *31* (15), 2008362.
- (40) Li, J.; Zhang, W.; Luo, X.; Wang, X.; Deng, W.; Wang, S.; Zhao, M.; Zhao, Q. A comparison between mesoporous and nonporous polydopamine as nanoplatfoms for synergistic chemo-photothermal therapy. *Colloids Surf., A* **2022**, *653*, 130005.
- (41) Yang, Y.; Fan, X.; Li, L.; Yang, Y.; Nuemisha, A.; Xue, D.; He, C.; Qian, J.; Hu, Q.; Chen, H.; et al. Semiconducting Polymer Nanoparticles as Theranostic System for Near-Infrared-II Fluorescence Imaging and Photothermal Therapy under Safe Laser Fluence. *ACS Nano* **2020**, *14* (2), 2509–2521.
- (42) Tousian, B.; Ghasemi, M. H.; Khosravi, A. R. Targeted chitosan nanoparticles embedded into graphene oxide functionalized with caffeic acid as a potential drug delivery system: New insight into cancer therapy. *Int. J. Biol. Macromol.* **2022**, *222*, 295–304.
- (43) Zhao, S.; Yan, L.; Cao, M.; Huang, L.; Yang, K.; Wu, S.; Lan, M.; Niu, G.; Zhang, W. Near-Infrared Light-Triggered Lysosome-Targetable Carbon Dots for Photothermal Therapy of Cancer. *ACS Appl. Mater. Interfaces* **2021**, *13* (45), 53610–53617.
- (44) Khakbaz, F.; Mirzaei, M.; Mahani, M. Lecithin sensitized thermo-sensitive niosome using NIR-carbon dots for breast cancer combined chemo-photothermal therapy. *J. Photochem. Photobiol., A* **2023**, *434*, 114236.
- (45) Consoli, G. M. L.; Giuffrida, M. L.; Zimbone, S.; Ferreri, L.; Maugeri, L.; Palmieri, M.; Satriano, C.; Forte, G.; Petralia, S. Green Light-Triggerable Chemo-Photothermal Activity of Cytarabine-Loaded Polymer Carbon Dots: Mechanism and Preliminary In Vitro Evaluation. *ACS Appl. Mater. Interfaces* **2023**, *15* (4), 5732–5743.
- (46) Kumar, A. V. P.; Dubey, S. K.; Tiwari, S.; Puri, A.; Hejmady, S.; Gorain, B.; Kesharwani, P. Recent advances in nanoparticles mediated photothermal therapy induced tumor regression. *Int. J. Pharm. (Amsterdam, Neth.)* **2021**, *606*, 120848.
- (47) Sheth, R. A.; Wen, X.; Li, J.; Melancon, M. P.; Ji, X.; Andrew Wang, Y.; Hsiao, C.-H.; Chow, D. S. L.; Whitley, E. M.; Li, C.; et al. Doxorubicin-loaded hollow gold nanospheres for dual photothermal ablation and chemoembolization therapy. *Cancer Nanotechnol.* **2020**, *11* (1), 1–16.
- (48) Li, Z.; Wang, S.; Zhao, J.; Luo, Y.; Liang, H.; Zhao, S.; Zhang, L. Gold Nanocluster Encapsulated Nanorod for Tumor Micro-

environment Simultaneously Activated NIR-II Photoacoustic/Photothermal Imaging and Cancer Therapy. *Adv. Ther. (Weinheim, Ger.)* **2023**, *6* (4), 2200350.

(49) Qiu, J.; Xie, M.; Wu, T.; Qin, D.; Xia, Y. Gold nanocages for effective photothermal conversion and related applications. *Chem. Sci.* **2020**, *11* (48), 12955–12973.

(50) Abbasi, J. Gold Nanoshells Ablate Prostate Tumors. *JAMA, J. Am. Med. Assoc.* **2019**, *322* (14), 1343–1343.

(51) Zheng, Z.; Yu, P.; Cao, H.; Cheng, M.; Zhou, T.; Lee, L. E.; Ulstrup, J.; Zhang, J.; Engelbrekt, C.; Ma, L. Starch Capped Atomically Thin CuS Nanocrystals for Efficient Photothermal Therapy. *Small* **2021**, *17* (47), 2103461.

(52) Zhang, W.; Ding, M.; Zhang, H.; Shang, H.; Zhang, A. Tumor acidity and near-infrared light responsive drug delivery MoS₂-based nanoparticles for chemo-photothermal therapy. *Photodiagn. Photodyn. Ther.* **2022**, *38*, 102716.

(53) Ajinkya, N.; Yu, X.; Kaithal, P.; Luo, H.; Somani, P.; Ramakrishna, S. Magnetic Iron Oxide Nanoparticle (IONP) Synthesis to Applications: Present and Future. *Materials* **2020**, *13* (20), 4644.

(54) Hu, R.; Fang, Y.; Huo, M.; Yao, H.; Wang, C.; Chen, Y.; Wu, R. Ultrasmall Cu₂-xS nanodots as photothermal-enhanced Fenton nanocatalysts for synergistic tumor therapy at NIR-II biowindow. *Biomaterials* **2019**, *206*, 101–114.

(55) Tran, H.-V.; Ngo, N. M.; Medhi, R.; Srinoi, P.; Liu, T.; Rittikulsittichai, S.; Lee, T. R. Multifunctional Iron Oxide Magnetic Nanoparticles for Biomedical Applications: A Review. *Materials* **2022**, *15* (2), 503.

(56) Zeng, P.; Hang, L.; Zhang, G.; Wang, Y.; Chen, Z.; Yu, J.; Zhang, T.; Cai, W.; Li, Y. Atom Absorption Energy Directed Symmetry-Breaking Synthesis of Au-Ag Hierarchical Nanostructures and Their Efficient Photothermal Conversion. *Small* **2022**, *18* (46), e2204748.

(57) Liu, Y.; Liang, Y.; Lei, P.; Zhang, Z.; Chen, Y. Multifunctional Superparticles for Magnetically Targeted NIR-II Imaging and Photodynamic Therapy. *Adv. Sci. (Weinheim, Ger.)* **2023**, *10* (2), e2203669.

(58) Wang, C.; Ye, X.; Zhao, Y.; Bai, L.; He, Z.; Tong, Q.; Xie, X.; Zhu, H.; Cai, D.; Zhou, Y.; et al. Cryogenic 3D printing of porous scaffolds for in situ delivery of 2D black phosphorus nanosheets, doxorubicin hydrochloride and osteogenic peptide for treating tumor resection-induced bone defects. *Biofabrication* **2020**, *12* (3), 035004.

(59) Venkateshalu, S.; Shariq, M.; Chaudhari, N. K.; Lee, K.; Grace, A. N. 2D non-carbide MXenes: an emerging material class for energy storage and conversion. *J. Mater. Chem. A* **2022**, *10* (38), 20174–20189.

(60) Liu, W.; Dong, A.; Wang, B.; Zhang, H. Current Advances in Black Phosphorus-Based Drug Delivery Systems for Cancer Therapy. *Adv. Sci. (Weinheim, Ger.)* **2021**, *8* (5), 2003033.

(61) Liu, H.; Xing, X.; Tan, Y.; Dong, H. Two-dimensional transition metal carbides and nitrides (MXenes) based biosensing and molecular imaging. *Nanophotonics* **2022**, *11* (22), 4977–4993.

(62) Yang, D.; Yang, G.; Yang, P.; Lv, R.; Gai, S.; Li, C.; He, F.; Lin, J. Assembly of Au Plasmonic Photothermal Agent and Iron Oxide Nanoparticles on Ultrathin Black Phosphorus for Targeted Photothermal and Photodynamic Cancer Therapy. *Adv. Funct. Mater.* **2017**, *27* (18), 1700371.

(63) Xiong, J.; Bian, Q.; Lei, S.; Deng, Y.; Zhao, K.; Sun, S.; Fu, Q.; Xiao, Y.; Cheng, B. Bi19S27I3 nanorods: a new candidate for photothermal therapy in the first and second biological near-infrared windows. *Nanoscale* **2021**, *13* (10), 5369–5382.

(64) Fernandes, N.; Rodrigues, C. F.; Moreira, A. F.; Correia, I. J. Overview of the application of inorganic nanomaterials in cancer photothermal therapy. *Biomater. Sci.* **2020**, *8* (11), 2990–3020.

(65) Zhang, Y.; Ning, R.; Wang, W.; Zhou, Y.; Chen, Y. Synthesis of Fe₃O₄/PDA Nanocomposites for Osteosarcoma Magnetic Resonance Imaging and Photothermal Therapy. *Front. Bioeng. Biotechnol.* **2022**, *10*, 844540.

(66) Francis, A. P.; Augustus, A. R.; Chandramohan, S.; Bhat, S. A.; Priya, V. V.; Rajagopalan, R. A review on biomaterials-based scaffold:

An emerging tool for bone tissue engineering. *Mater. Today Commun.* **2023**, *34*, 105124.

(67) Serrano-Aroca, A.; Cano-Vicent, A.; Sabater i Serra, R.; El-Tanani, M.; Aljabali, A.; Tambuwala, M. M.; Mishra, Y. K. Scaffolds in the microbial resistant era: Fabrication, materials, properties and tissue engineering applications. *Mater. Today Bio* **2022**, *16*, 100412.

(68) Li, L. F.; Hao, R. N.; Qin, J. J.; Song, J.; Chen, X. F.; Rao, F.; Zhai, J. L.; Zhao, Y.; Zhang, L. Q.; Xue, J. J. Electrospun Fibers Control Drug Delivery for Tissue Regeneration and Cancer Therapy. *Adv. Fiber Mater.* **2022**, *4* (6), 1375–1413.

(69) Smith, L. A.; Ma, P. X. Nano-fibrous scaffolds for tissue engineering. *Colloids Surf., B* **2004**, *39* (3), 125–131.

(70) El-Kady, A. M.; Rizk, R. A.; Abd El-Hady, B. M.; Shafaa, M. W.; Ahmed, M. M. Characterization, and antibacterial properties of novel silver releasing nanocomposite scaffolds fabricated by the gas foaming/salt-leaching technique. *J. Genet. Eng. Biotechnol.* **2012**, *10* (2), 229–238.

(71) Wang, N.; Zhou, Z.; Xia, L.; Dai, Y.; Liu, H. Fabrication and characterization of bioactive β -Ca₂SiO₄/PHBV composite scaffolds. *Mater. Sci. Eng., C* **2013**, *33* (4), 2294–2301.

(72) Serrano-Aroca, A.; Llorens-Gómez, M. Dynamic mechanical analysis and water vapour sorption of highly porous poly(methyl methacrylate). *Polymer* **2017**, *125*, 58–65.

(73) Shi, X.; Wang, Y.; Ren, L.; Zhao, N.; Gong, Y.; Wang, D.-A. Novel mesoporous silica-based antibiotic releasing scaffold for bone repair. *Acta Biomater.* **2009**, *5* (5), 1697–1707.

(74) Li, J.; Li, L.; Zhou, J.; Zhou, Z.; Wu, X.-L.; Wang, L.; Yao, Q. 3D printed dual-functional biomaterial with self-assembly micro-nano surface and enriched nano argentine for antibacterial and bone regeneration. *Applied Materials Today* **2019**, *17*, 206–215.

(75) Llorens-Gómez, M.; Salesa, B.; Serrano-Aroca, A. Physical and biological properties of alginate/carbon nanofibers hydrogel films. *Int. J. Biol. Macromol.* **2020**, *151*, 499–507.

(76) Santos-Rosales, V.; Ardao, I.; Goimil, L.; Gomez-Amoza, J. L.; Garcia-Gonzalez, C. A. Solvent-Free Processing of Drug-Loaded Poly(ϵ -Caprolactone) Scaffolds with Tunable Macroporosity by Combination of Supercritical Foaming and Thermal Porogen Leaching. *Polymers (Basel, Switz.)* **2021**, *13* (1), 159.

(77) Khan, M. U. A.; Al-Thebaiti, M. A.; Hashmi, M. U.; Aftab, S.; Abd Razak, S. I.; Abu Hassan, S.; Kadir, M. R.; Amin, R. Synthesis of Silver-Coated Bioactive Nanocomposite Scaffolds Based on Grafted Beta-Glucan/Hydroxyapatite via Freeze-Drying Method: Anti-Microbial and Biocompatibility Evaluation for Bone Tissue Engineering. *Polymers (Basel, Switz.)* **2020**, *13* (4), 971.

(78) Yang, D.-L.; Faraz, F.; Wang, J.-X.; Radacsi, N. Combination of 3D Printing and Electrospinning Techniques for Biofabrication. *Adv. Mater. Technol. (Weinheim, Ger.)* **2022**, *7* (7), 2101309.

(79) Wei, C.; Jin, X.; Wu, C.; Zhang, W. Injectable composite hydrogel based on carbon particles for photothermal therapy of bone tumor and bone regeneration. *J. Mater. Sci. Technol. (Shenyang, China)* **2022**, *118*, 64–72.

(80) Yu, T.; Hu, Y.; He, W.; Xu, Y.; Zhan, A.; Chen, K.; Liu, M.; Xiao, X.; Xu, X.; Feng, Q.; et al. An injectable and self-healing hydrogel with dual physical crosslinking for in-situ bone formation. *Mater. Today Bio* **2023**, *19*, 100558.

(81) Yang, Z.; Xue, J.; Li, T.; Zhai, D.; Yu, X.; Huan, Z.; Wu, C. 3D printing of sponge spicules-inspired flexible bioceramic-based scaffolds. *Biofabrication* **2022**, *14* (3), 035009.

(82) Feng, B.; Zhang, M.; Qin, C.; Zhai, D.; Wang, Y.; Zhou, Y.; Chang, J.; Zhu, Y.; Wu, C. 3D printing of conch-like scaffolds for guiding cell migration and directional bone growth. *Bioact. Mater.* **2023**, *22*, 127–140.

(83) Yu, X.; Wang, Y.; Zhang, M.; Ma, H.; Feng, C.; Zhang, B.; Wang, X.; Ma, B.; Yao, Q.; Wu, C. 3D printing of gear-inspired biomaterials: Immunomodulation and bone regeneration. *Acta Biomater.* **2023**, *156*, 222–233.

(84) Hamidi, S.; Monajjemzadeh, F.; Siah-Shadbad, M.; Khatibi, S. A.; Farjami, A. Antibacterial activity of natural polymer gels and

- potential applications without synthetic antibiotics. *Polym. Eng. Sci.* **2023**, *63* (1), 5–21.
- (85) Terzopoulou, Z.; Zamboulis, A.; Koumentakou, I.; Michailidou, G.; Noordam, M. J.; Bikiaris, D. N. Biocompatible Synthetic Polymers for Tissue Engineering Purposes. *Biomacromolecules* **2022**, *23* (5), 1841–1863.
- (86) Sarfaraz, S.; Khan, A.; Hameed, F.; Arshad, A.; Mutahir, Z.; Zeeshan, R.; Ijaz, K.; Chaudhry, A. A.; Khalid, H.; Rehman, I.; et al. Osteogenic and antibacterial scaffolds of silk fibroin/Ce-doped ZnO for bone tissue engineering. *Int. J. Polym. Mater. Polym. Biomater.* **2023**, *72* (15), 1205–1216.
- (87) Chen, Q.; Shan, X.; Shi, S.; Jiang, C.; Li, T.; Wei, S.; Zhang, X.; Sun, G.; Liu, J. Tumor microenvironment-responsive polydopamine-based core/shell nanoplatfor for synergetic theranostics. *J. Mater. Chem. B* **2020**, *8* (18), 4056–4066.
- (88) Massoumi, B.; Abbasian, M.; Jahanban-Esfahlan, R.; Mohammad-Rezaei, R.; Khalilzadeh, B.; Samadian, H.; Rezaei, A.; Derakhshankhah, H.; Jaymand, M. A novel bio-inspired conductive, biocompatible, and adhesive terpolymer based on polyaniline, polydopamine, and polylactide as scaffolding biomaterial for tissue engineering application. *Int. J. Biol. Macromol.* **2020**, *147*, 1174–1184.
- (89) Meng, Z.; Liu, Y.; Xu, K.; Sun, X.; Yu, Q.; Wu, Z.; Zhao, Z. Biomimetic Polydopamine-Modified Silk Fibroin/Curcumin Nanofibrous Scaffolds for Chemo-photothermal Therapy of Bone Tumor. *ACS Omega* **2021**, *6* (34), 22213–22223.
- (90) Miao, H.; Shen, R.; Zhang, W.; Lin, Z.; Wang, H.; Yang, L.; Liu, X.-Y.; Lin, N. Near-Infrared Light Triggered Silk Fibroin Scaffold for Photothermal Therapy and Tissue Repair of Bone Tumors. *Adv. Funct. Mater.* **2021**, *31* (10), 2007188.
- (91) Yuan, B.; Zhou, X.; Li, Y.; Zhao, Y.; Xue, M.; Guo, Q.; Zheng, G.; Chen, X.; Lin, H.; Guo, X. Black-Phosphorus-Nanosheet-Reinforced Coating of Implants for Sequential Biofilm Ablation and Bone Fracture Healing Acceleration. *ACS Appl. Mater. Interfaces* **2022**, *14* (41), 47036–47051.
- (92) Ma, L.; Feng, X.; Liang, H.; Wang, K.; Song, Y.; Tan, L.; Wang, B.; Luo, R.; Liao, Z.; Li, G.; et al. A novel photothermally controlled multifunctional scaffold for clinical treatment of osteosarcoma and tissue regeneration. *Mater. Today* **2020**, *36*, 48–62.
- (93) Lu, Y.; Li, L.; Li, M.; Lin, Z.; Wang, L.; Zhang, Y.; Yin, Q.; Xia, H.; Han, G. Zero-Dimensional Carbon Dots Enhance Bone Regeneration, Osteosarcoma Ablation, and Clinical Bacterial Eradication. *Bioconjugate Chem.* **2018**, *29* (9), 2982–2993.
- (94) Dang, W.; Ma, B.; Li, B.; Huan, Z.; Ma, N.; Zhu, H.; Chang, J.; Xiao, Y.; Wu, C. 3D printing of metal-organic framework nanosheets-structured scaffolds with tumor therapy and bone construction. *Biofabrication* **2020**, *12* (2), 025005.
- (95) Ma, H.; Jiang, C.; Zhai, D.; Luo, Y.; Chen, Y.; Lv, F.; Yi, Z.; Deng, Y.; Wang, J.; Chang, J.; et al. A Bifunctional Biomaterial with Photothermal Effect for Tumor Therapy and Bone Regeneration. *Adv. Funct. Mater.* **2016**, *26* (8), 1197–1208.
- (96) Zhang, Y.; Zhai, D.; Xu, M.; Yao, Q.; Chang, J.; Wu, C. 3D-printed bioceramic scaffolds with a Fe₃O₄/graphene oxide nanocomposite interface for hyperthermia therapy of bone tumor cells. *J. Mater. Chem. B* **2016**, *4* (17), 2874–2886.
- (97) Zhao, Q.; Shi, M.; Yin, C.; Zhao, Z.; Zhang, J.; Wang, J.; Shen, K.; Zhang, L.; Tang, H.; Xiao, Y.; et al. Dual-Wavelength Photosensitive Nano-in-Micro Scaffold Regulates Innate and Adaptive Immune Responses for Osteogenesis. *Nano-Micro Lett.* **2021**, *13* (1), 1–20.
- (98) Dang, W.; Li, T.; Li, B.; Ma, H.; Zhai, D.; Wang, X.; Chang, J.; Xiao, Y.; Wang, J.; Wu, C. A bifunctional scaffold with CuFeSe₂ nanocrystals for tumor therapy and bone reconstruction. *Biomaterials* **2018**, *160*, 92–106.
- (99) Wang, H.; Zeng, X.; Pang, L.; Wang, H.; Lin, B.; Deng, Z.; Qi, E. L. X.; Miao, N.; Wang, D.; Huang, P.; et al. Integrative treatment of anti-tumor/bone repair by combination of MoS₂ nanosheets with 3D printed bioactive borosilicate glass scaffolds. *Chem. Eng. J. (Amsterdam, Neth.)* **2020**, *396*, 125081.
- (100) Du, J.; Ding, H.; Fu, S.; Li, D.; Yu, B. Bismuth-coated 80S15C bioactive glass scaffolds for photothermal antitumor therapy and bone regeneration. *Front. Bioeng. Biotechnol.* **2023**, *10*, 1098923.
- (101) Pan, T.; Fu, W.; Xin, H.; Geng, S.; Li, Z.; Cui, H.; Zhang, Y.; Chu, P. K.; Zhou, W.; Yu, X.-F. Calcium Phosphate Mineralized Black Phosphorous with Enhanced Functionality and Anticancer Bioactivity. *Adv. Funct. Mater.* **2020**, *30* (38), 2003069.
- (102) Dang, W.; Jin, Y.; Yi, K.; Ju, E.; Zhuo, C.; Wei, H.; Wen, X.; Wang, Y.; Li, M.; Tao, Y. Hemin particles-functionalized 3D printed scaffolds for combined photothermal and chemotherapy of osteosarcoma. *Chem. Eng. J. (Amsterdam, Neth.)* **2021**, *422*, 129919.
- (103) Wang, L.; Yang, Q.; Huo, M.; Lu, D.; Gao, Y.; Chen, Y.; Xu, H. Engineering Single-Atomic Iron-Catalyst-Integrated 3D-Printed Bioscaffolds for Osteosarcoma Destruction with Antibacterial and Bone Defect Regeneration Bioactivity. *Adv. Mater.* **2021**, *33* (31), 2100150.
- (104) Ma, H.; Li, T.; Huan, Z.; Zhang, M.; Yang, Z.; Wang, J.; Chang, J.; Wu, C. 3D printing of high-strength bioscaffolds for the synergistic treatment of bone cancer. *NPG Asia Mater.* **2018**, *10*, 31–44.
- (105) Dong, S.; Chen, Y.; Yu, L.; Lin, K.; Wang, X. Magnetic Hyperthermia-Synergistic H₂O₂ Self-Sufficient Catalytic Suppression of Osteosarcoma with Enhanced Bone-Regeneration Bioactivity by 3D-Printing Composite Scaffolds. *Adv. Funct. Mater.* **2020**, *30* (4), 1907071.
- (106) Zhuang, H.; Qin, C.; Zhang, M.; Ma, J.; Zhai, D.; Ma, B.; Ma, N.; Huan, Z.; Wu, C. 3D-printed bioceramic scaffolds with Fe₃S₄ microflowers for magnetothermal and chemodynamic therapy of bone tumor and regeneration of bone defects. *Biofabrication* **2021**, *13* (4), 045010.
- (107) Zhao, C.; Shen, A.; Zhang, L.; Lin, K.; Wang, X. Borocarbonitrides nanosheets engineered 3D-printed scaffolds for integrated strategy of osteosarcoma therapy and bone regeneration. *Chem. Eng. J. (Amsterdam, Neth.)* **2020**, *401*, 125989.
- (108) Yang, C.; Ma, H.; Wang, Z.; Younis, M. R.; Liu, C.; Wu, C.; Luo, Y.; Huang, P. 3D Printed Wesselsite Nanosheets Functionalized Scaffold Facilitates NIR-II Photothermal Therapy and Vascularized Bone Regeneration. *Adv. Sci. (Weinheim, Ger.)* **2021**, *8* (20), e2100894.
- (109) Long, J.; Zhang, W.; Chen, Y.; Teng, B.; Liu, B.; Li, H.; Yao, Z.; Wang, D.; Li, L.; Yu, X.-F.; et al. Multifunctional magnesium incorporated scaffolds by 3D-Printing for comprehensive postsurgical management of osteosarcoma. *Biomaterials* **2021**, *275*, 120950.
- (110) Lin, H.; Shi, S.; Lan, X.; Quan, X.; Xu, Q.; Yao, G.; Liu, J.; Shuai, X.; Wang, C.; Li, X.; et al. Scaffold 3D-Printed from Metallic Nanoparticles-Containing Ink Simultaneously Eradicates Tumor and Repairs Tumor-Associated Bone Defects. *Small Methods* **2021**, *5* (9), e2100536.
- (111) Lee, J.-H.; Uyama, H.; Kwon, O.-K.; Kim, Y.-J. Nitric oxide and reactive oxygen species-releasing polylactic acid monolith for enhanced photothermal therapy of osteosarcoma. *J. Ind. Eng. Chem. (Amsterdam, Neth.)* **2021**, *94*, 498–506.
- (112) Samadian, H.; Khastar, H.; Ehterami, A.; Salehi, M. Bioengineered 3D nanocomposite based on gold nanoparticles and gelatin nanofibers for bone regeneration: in vitro and in vivo study. *Sci. Rep.* **2021**, *11* (1), 1–11.
- (113) Wang, D.; Wang, W.; Lu, H.; You, C.; Liang, L.; Liu, C.; Xiang, H.; Chen, Y. Charge transfer of ZnTPP/C60 cocrystal-hybridized bioimplants satisfies osteosarcoma eradication with antitumoral, antibacterial and osteogenic performances. *Nano Today* **2022**, *46*, 101562.
- (114) Zhao, Y.; Peng, X.; Xu, X.; Wu, M.; Sun, F.; Xin, Q.; Zhang, H.; Zuo, L.; Cao, Y.; Xia, Y.; et al. Chitosan based photothermal scaffold fighting against bone tumor-related complications: Recurrence, infection, and defects. *Carbohydr. Polym.* **2023**, *300*, 120264.
- (115) Xu, C.; Ma, B.; Peng, J.; Gao, L.; Xu, Y.; Huan, Z.; Chang, J. Tricalcium silicate/graphene oxide bone cement with photothermal properties for tumor ablation. *J. Mater. Chem. B* **2019**, *7* (17), 2808–2818.

- (116) Yin, J.; Han, Q.; Zhang, J.; Liu, Y.; Gan, X.; Xie, K.; Xie, L.; Deng, Y. MXene-Based Hydrogels Endow Polyetheretherketone with Effective Osteogenicity and Combined Treatment of Osteosarcoma and Bacterial Infection. *ACS Appl. Mater. Interfaces* **2020**, *12* (41), 45891–45903.
- (117) Wang, X.; Zhai, D.; Yao, X.; Wang, Y.; Ma, H.; Yu, X.; Du, L.; Lin, H.; Wu, C. 3D printing of pink bioceramic scaffolds for bone tumor tissue therapy. *Applied Materials Today* **2022**, *27*, 101443.
- (118) Dang, W.; Yi, K.; Ju, E.; Jin, Y.; Xu, Y.; Wang, H.; Chen, W.-C.; Wang, K.; Wang, Y.; Tao, Y.; et al. 3D Printed Bioceramic Scaffolds as a Universal Therapeutic Platform for Synergistic Therapy of Osteosarcoma. *ACS Appl. Mater. Interfaces* **2021**, *13* (16), 18488–18499.
- (119) He, C.; Yu, L.; Yao, H.; Chen, Y.; Hao, Y. Combinatorial Photothermal 3D Printing Scaffold and Checkpoint Blockade Inhibits Growth/Metastasis of Breast Cancer to Bone and Accelerates Osteogenesis. *Adv. Funct. Mater.* **2021**, *31* (10), 2006214.
- (120) Huang, Y.; Du, Z.; Li, K.; Jing, W.; Wei, P.; Zhao, B.; Yu, Y.; Cai, Q.; Yang, X. ROS-Scavenging Electroactive Polyphosphazene-Based Core-Shell Nanofibers for Bone Regeneration. *Adv. Fiber Mater.* **2022**, *4* (4), 894–907.
- (121) Wang, S.; Wang, F.; Zhao, X.; Yang, F.; Xu, Y.; Yan, F.; Xia, D.; Liu, Y. The effect of near-infrared light-assisted photothermal therapy combined with polymer materials on promoting bone regeneration: A systematic review. *Mater. Des.* **2022**, *217*, 110621.
- (122) Liu, S.; Han, Z.; Hao, J.-N.; Zhang, D.; Li, X.; Cao, Y.; Huang, J.; Li, Y. Engineering of a NIR-activable hydrogel-coated mesoporous bioactive glass scaffold with dual-mode parathyroid hormone derivative release property for angiogenesis and bone regeneration. *Bioact. Mater.* **2023**, *26*, 1–13.
- (123) Zhou, J.; Zhang, Z.; Joseph, J.; Zhang, X.; Ferdows, B. E.; Patel, D. N.; Chen, W.; Banfi, G.; Molinaro, R.; Cosco, D.; et al. Biomaterials and nanomedicine for bone regeneration: Progress and future prospects. *Exploration (Beijing, China)* **2021**, *1* (2), 20210011.
- (124) Xue, X.; Zhang, H.; Liu, H.; Wang, S.; Li, J.; Zhou, Q.; Chen, X.; Ren, X.; Jing, Y.; Deng, Y.; et al. Rational Design of Multifunctional CuS Nanoparticle PEG Composite Soft Hydrogel Coated 3D Hard Polycaprolactone Scaffolds for Efficient Bone Regeneration. *Adv. Funct. Mater.* **2022**, *32* (33), 2202470.
- (125) Li, Q.; Liu, W.; Hou, W.; Wu, X.; Wei, W.; Liu, J.; Hu, Y.; Dai, H. Micropatterned photothermal double-layer periosteum with angiogenesis-neurogenesis coupling effect for bone regeneration. *Mater. Today Bio* **2023**, *18*, 100536.
- (126) Zhang, X.; Li, Q.; Li, L.; Ouyang, J.; Wang, T.; Chen, J.; Hu, X.; Ao, Y.; Qin, D.; Zhang, L.; et al. Bioinspired Mild Photothermal Effect-Reinforced Multifunctional Fiber Scaffolds Promote Bone Regeneration. *ACS Nano* **2023**, *17* (7), 6466–6479.
- (127) Xu, X.; Chen, X.; Wang, H.; Mei, X.; Chen, B.; Li, R.; Qin, Y. Balancing the toxicity, photothermal effect, and promotion of osteogenesis: Photothermal scaffolds for malignant bone tumor therapy. *Mater. Today Adv.* **2022**, *13*, 100209.
- (128) Huang, B.; Yin, Z.; Zhou, F.; Su, J. Functional anti-bone tumor biomaterial scaffold: construction and application. *J. Mater. Chem. B* **2023**, *11* (36), 8565–8585.
- (129) Xiong, Y.; Mi, B.-B.; Lin, Z.; Hu, Y.-Q.; Yu, L.; Zha, K.-K.; Panayi, A. C.; Yu, T.; Chen, L.; Liu, Z.-P.; et al. The role of the immune microenvironment in bone, cartilage, and soft tissue regeneration: from mechanism to therapeutic opportunity. *Mil. Med. Res.* **2022**, *9* (1), 65.
- (130) Zhang, G.; Lu, Y.; Song, J.; Huang, D.; An, M.; Chen, W.; Han, P.; Yao, X.; Zhang, X. A multifunctional nano-hydroxyapatite/MXene scaffold for the photothermal/dynamic treatment of bone tumours and simultaneous tissue regeneration. *J. Colloid Interface Sci.* **2023**, *652*, 1673–1684.
- (131) Pektas, H. K.; Demidov, Y.; Ahvan, A.; Abie, N.; Georgieva, V. S.; Chen, S.; Farè, S.; Brachvogel, B.; Mathur, S.; Maleki, H. MXene-Integrated Silk Fibroin-Based Self-Assembly-Driven 3D-Printed Theragenerative Scaffolds for Remotely Photothermal Anti-Osteo-
- sarcoma Ablation and Bone Regeneration. *ACS Mater. Au* **2023**, *3*, 711.
- (132) Luo, Y.; Liu, H.; Zhang, Y.; Liu, Y.; Liu, S.; Liu, X.; Luo, E. Metal ions: the unfading stars of bone regeneration—from bone metabolism regulation to biomaterial applications. *Biomater. Sci.* **2023**, *11*, 7268.
- (133) Liu, Y.; Li, T.; Ma, H.; Zhai, D.; Deng, C.; Wang, J.; Zhuo, S.; Chang, J.; Wu, C. 3D-printed scaffolds with bioactive elements-induced photothermal effect for bone tumor therapy. *Acta Biomater.* **2018**, *73*, 531–546.
- (134) Zhang, X.; Wei, H.; Dong, C.; Wang, J.; Zhang, T.; Huang, L.; Ni, D.; Luo, Y. 3D printed hydrogel/bioceramics core/shell scaffold with NIR-II triggered drug release for chemo-photothermal therapy of bone tumors and enhanced bone repair. *Chem. Eng. J. (Amsterdam, Neth.)* **2023**, *461*, 141855.
- (135) Gu, J.; Liu, X.; Cui, P.; Yi, X. Multifunctional bioactive glasses with spontaneous degradation for simultaneous osteosarcoma therapy and bone regeneration. *Biomater. Adv.* **2023**, *154*, 213626.
- (136) Kong, Y.; Zhou, L.; Liao, S.; Wang, C.; Chen, J.; Cai, X.; Zhao, S.; Song, D.; Zhang, Y. Dual peptide-engineered and gadolinium-doped polydopamine particles as targeted nanotheranostics for the treatment of osteosarcoma and related osteolysis. *Chem. Eng. J. (Amsterdam, Neth.)* **2022**, *444*, 136516.